



HAL
open science

Novel UBQLN2 mutations linked to Amyotrophic Lateral Sclerosis and atypical Hereditary Spastic Paraplegia phenotype through defective HSP70-mediated proteolysis

Elisa Teyssou, Laura Chartier, Maria-Del-Mar Amador, Roselina Lam, Géraldine Lautrette, Marie Nicol, Selma Machat, Sandra da Barroca, Carine Moigneu, Mathilde Mairey, et al.

► To cite this version:

Elisa Teyssou, Laura Chartier, Maria-Del-Mar Amador, Roselina Lam, Géraldine Lautrette, et al.. Novel UBQLN2 mutations linked to Amyotrophic Lateral Sclerosis and atypical Hereditary Spastic Paraplegia phenotype through defective HSP70-mediated proteolysis. *Neurobiology of Aging*, 2017, 58, pp.239.e11-239.e20. 10.1016/j.neurobiolaging.2017.06.018 . hal-03001781

HAL Id: hal-03001781

<https://hal.science/hal-03001781>

Submitted on 12 Nov 2020

HAL is a multi-disciplinary open access archive for the deposit and dissemination of scientific research documents, whether they are published or not. The documents may come from teaching and research institutions in France or abroad, or from public or private research centers.

L'archive ouverte pluridisciplinaire **HAL**, est destinée au dépôt et à la diffusion de documents scientifiques de niveau recherche, publiés ou non, émanant des établissements d'enseignement et de recherche français ou étrangers, des laboratoires publics ou privés.

Novel *UBQLN2* mutations linked to Amyotrophic Lateral Sclerosis and atypical Hereditary Spastic Paraplegia phenotype through defective HSP70-mediated proteolysis

Elisa Teyssou^{1*}, Laura Chartier^{1*}, Maria-Del-Mar Amador², Roselina Lam¹, Géraldine Lautrette³, Marie Nicol³, Selma Machat³, Sandra Da Barroca¹, Carine Moigneu¹, Mathilde Mairey^{1,4}, Thierry Larmonier⁵, Safaa Saker⁵, Christelle Dussert¹, Sylvie Forlani¹, Bertrand Fontaine^{1,2}, Danielle Seilhean^{1,6}, Delphine Bohl¹, Séverine Boillée¹, Vincent Meininger^{2,7}, Philippe Couratier³, François Salachas^{1,2}, Giovanni Stevanin^{1,4,8}, Stéphanie Millecamps^{1#}

¹Inserm U1127, CNRS UMR7225, Sorbonne Universités, UPMC Univ Paris 6 UMRS1127, Institut du Cerveau et de la Moelle épinière, ICM, 75013 Paris, France

²Département de Neurologie, Assistance Publique Hôpitaux de Paris (APHP), Centre de ressources et de compétences SLA Ile de France, Hôpital de la Pitié-Salpêtrière, 75013 Paris, France

³Service de Neurologie, Centre de ressources et de compétences SLA, CHU Dupuytren, 87000 Limoges, France

⁴Ecole Pratique des Hautes Etudes, EPHE, Université de recherche Paris Sciences et Lettres, 75014, Paris, France.

⁵Banque d'ADN et de cellules du Généthon, 91000 Evry, France

⁶Département de Neuropathologie, APHP, Hôpital Pitié-Salpêtrière, 75013 Paris, France

⁷Hôpital des Peupliers, Ramsay Générale de Santé, 75013 Paris, France

⁸Centre de Référence de Neurogénétique, Fédération de Génétique, APHP, Hôpital Pitié-Salpêtrière, 75013 Paris, France

* ET and LC contributed equally

#To whom correspondence should be addressed: Dr Stéphanie Millecamps, Institut du Cerveau et de la Moelle épinière, Hôpital Pitié-Salpêtrière, 47-83 Bd de l'Hôpital, CS21414, 75646 Paris Cedex, France, tel : 33157274341, e-mail: stephanie.millecamps@upmc.fr

Abstract

Mutations in *UBQLN2* have been associated with rare cases of X-linked juvenile and adult forms of Amyotrophic Lateral Sclerosis (ALS) and ALS linked to Frontotemporal Dementia (FTD). Here we report one known (c.1489C>T, p.Pro497Ser, P497S) and three novel (c.1481C>T, p.Pro494Leu, P494L; c.1498C>T, p.Pro500Ser, P500S and c.1516C>G, p.Pro506Ala, P506A) missense mutations in the PXX domain of *UBQLN2* in familial motor neuron diseases including ALS and spastic paraplegia. One novel missense mutation (c.1462G>A, p.Ala488Thr, A488T) adjacent to this hot spot *UBQLN2* domain was identified in a sporadic case of ALS. These mutations are conserved in mammals, are absent from ExAC and gnomAD browsers and are predicted to be deleterious by SIFT *in silico* analysis. Patient lymphoblasts carrying a *UBQLN2* mutation showed absence of ubiquilin-2 accumulation, disrupted binding with HSP70 and impaired autophagic pathway. Our results confirm the role of PXX repeat in ALS pathogenesis, show that *UBQLN2* linked disease can manifest like a spastic paraplegia phenotype, evidence a highly reduced disease penetrance in females carrying *UBQLN2* mutations, which is important information for genetic counseling and underline the pivotal role of ubiquilin-2 in proteolysis regulation pathways.

Key words: Motor neuron disease, X-linked ALS, FTD, proteolysis regulation, incomplete penetrance, X inactivation, dimerization.

Abbreviations: ALS: Amyotrophic Lateral Sclerosis, ERAD: endoplasmic reticulum-associated protein degradation; FALS: familial ALS; FTD: Frontotemporal Dementia; HSP70: heat-shock protein 70 kDa; SALS: Sporadic ALS; SP: Spastic Paraplegia; UBA: ubiquitin-associated domain; UBL: ubiquitin-like domain; UIM: ubiquitin-interacting motifs, UPS: ubiquitin-proteasome system.

Disclosure statement.

The authors declare no actual or potential conflicts of interest.

1. Introduction

Mutations in *UBQLN2*, an intronless gene located on the X chromosome which encodes ubiquilin-2, have been identified in families with dominant X-linked juvenile and adult-onset amyotrophic lateral sclerosis (ALS) and/or frontotemporal dementia (FTD) (Deng et al., 2011). Ubiquilin-2 is a component of the ubiquitin inclusions detected in degenerating neurons in ALS patients carrying or not a mutation in the *UBQLN2* gene, which suggests a role for this protein in a final common pathway mediating motor neuron degeneration (Deng et al., 2011). Ubiquilin-2 (also known as PLIC-2 or CHAP1) contains four main domains. The N-terminal sequence called the ubiquitin-like domain (UBL) is very similar to ubiquitin and binds to ubiquitin-interacting motifs (UIM) expressed by proteasomes and endocytic receptors degraded by lysosomes (Hofmann and Falquet, 2001; Walters et al., 2002). The central domain contains 4 co-chaperone-like regions with homology to STI1 (which binds to Stch, a protein similar to HSP70). There are also the proline/glycine repeat (12 PXX tandem repeat) and a conserved C-terminal domain called the ubiquitin-associated domain (UBA) (Kaye et al., 2000). These protein domains are shared by the three other members of ubiquilin family (ubiquilin-1, -3 and -4) except the proline/glycine repeat which is unique to ubiquilin-2.

UBQLN2 regulates several protein degradation pathways including the ubiquitin-proteasome system (UPS), the endoplasmic reticulum-associated protein degradation (ERAD) pathway and macroautophagy. Indeed, *UBQLN2* can bind to the polyubiquitinated proteins through its UBA domain and can deliver them to the proteasome through interaction with its UBL domain (Walters et al., 2002; Kleijnen et al., 2003; Ko et al., 2004). *UBQLN2* is also thought to address ERAD substrates to the proteasome since it was shown to interact with *UBXD8* and *HERPUD1*, both involved in removal of improperly folded newly synthesized proteins (Kim et al., 2008; Xia et al., 2014). *UBQLN2* was also recently shown to bind heat-shock proteins including HSP70 (encoded by *HSPA1A*) and to deliver ubiquitinated client-bound HSP70 proteins to the proteasome (Hjerpe et al., 2016). Therefore, defects in these processes could contribute to accumulation of aggregated and/or misfolded proteins in ALS

disease. In addition, ubiquilin proteins were reported to regulate macroautophagy in which cytosolic cargo is packaged in a double-membrane structure (autophagosome) that fuses with lysosomes harboring the acid hydrolases involved in protein degradation (N'Diaye et al., 2009). Co-immunoprecipitation studies showed that ubiquilin-1 and -2 were components of a complex with polyubiquitinated proteins and microtubule-associated protein 1 light chain 3 (LC3) involved in the formation of autophagosomes (Rothenberg et al., 2010).

Intriguingly, 7 different *UBQLN2* mutations identified in ALS patients involved one proline residue of the unique 12 PXX tandem repeat domain of the protein (Deng et al., 2011; Gellera et al., 2013; Vengoechea et al., 2013; Fahed et al., 2014; Ozoguz et al., 2015) and other mutations were identified on adjacent residues (Williams et al., 2012; Gellera et al., 2013) underlying the relevance of this domain for ALS pathogenesis. Whole exome sequencing analyses conducted on familial ALS (FALS) index cases and controls (1,022 FALS and 7,315 controls) revealed that *UBQLN2* has a study-wide significant enrichment of rare variants in FALS cases compared to controls, ranking this gene third after *SOD1* and *TARDBP*, when excluding FALS cases harboring a repeat expansion in the *C9orf72* gene (Kenna et al., 2016). These data underlined that *UBQLN2* contributes to a significant proportion of FALS.

We previously reported the genetic analyses of a population of 130 French FALS patients and 240 sporadic ALS (SALS) without finding any causative *UBQLN2* mutation (Millecamps et al., 2012a). In the present study we analyzed 850 additional ALS patients (285 FALS and 565 SALS) and identified 5 *UBQLN2* mutations, including 4 novel ones, for which we explored the possible consequences on protein degrading pathways.

2. Material and Methods

2.1. Genetic analyses.

All participants signed a consent form for the genetic research and protocols were approved by the Medical Research Ethics Committee of "Assistance Publique-Hôpitaux de Paris". The diagnosis of ALS,

spastic paraplegia (SP) and FTD were based on published criteria (Brooks et al., 2000; Gasser et al., 2010; Rascovsky et al., 2011).

We systematically sequenced by Sanger analysis a region of 390 pb spanning the PXX repeat domain of *UBQLN2* in 415 FALS and 805 SALS in order to find possible novel *UBQLN2* mutations causing ALS and/or concurrent *UBQLN2* variants in patients carrying a mutation in the other ALS genes using a procedure described previously (Millecamps et al., 2012a). The entire *UBQLN2* gene sequence was further analyzed in patients with an identified *UBQLN2* mutation in this region to ensure that positive patients carry only one mutation in this gene. All these ALS patients were also systematically screened for *C9orf72* expansion and *SOD1*, *TARDBP* and *FUS* mutations (Millecamps et al., 2012b).

For patients presenting SP, we used a panel covering 210,363 bases corresponding to 1001 regions of 70 genes (Table S1) known to be responsible for dominant and recessive hereditary SP forms (Tesson et al., 2015). The procedure consisted in a customized ROCHE/Nimblegen capture followed by massive parallel 75 bp sequencing on MiSeq apparatus (Illumina).

Before sequencing cDNA, total RNAs were extracted from lymphoblasts using the Trizol reagent (Life Technologies), subjected to RNase-free DNase treatment (Qiagen) and purified using RNeasy columns (Qiagen). First-Strand cDNA synthesis was performed using ThermoScript RT-PCR system (Life Technologies) according to the manufacturer's instructions.

2.2. Lymphoblast cultures.

Lymphoblastoid cell lines from the ALS patients carrying the P494L, P497S or the P506A mutation were established by Epstein Barr virus transformation of peripheral blood mononuclear cells. Lymphoblasts from age-matched healthy men were used as controls. Lymphoblasts were grown in RPMI 1640 supplemented with 10% fetal bovine serum, 50 U/ml penicillin and 50 mg/ml streptomycin (Life Technologies) renewed twice a week. Lymphoblasts ($5 \cdot 10^6$ cells) were treated with 5 mM of NH_4Cl (Sigma-Aldrich) during 1 hour at 37°C for lysosomal degradation inactivation and incubated at 42°C

during 2 hours for heat-shock induction. For pellets, they were centrifuged 5 min at 3,000 rpm, rinsed in phosphate buffered saline (PBS) solution and frozen at -80°C.

2.3. Antibodies.

Primary antibodies against ubiquilin 2 (NBP2-25164, Novus Biologicals), HSP70 (MAB3516, Merck Millipore), p62 (MABC32, Merck Millipore) and nuclei clone 235-1 (MAB1281, Merck Millipore) were from mouse and those against LC3B (NB100-2220, Novus Biologicals) and GAPDH (D16H11, Cell Signaling Technology) from rabbit. Peroxidase-conjugated secondary antibodies were goat anti-rabbit or anti-mouse with minimal cross-reaction to human serum proteins (Jackson Immunoresearch Laboratories).

2.4. Western Blot analysis.

For immunoblots, cell pellets were homogenized in 50 mM Tris-HCl pH8, 150 mM NaCl, 1 mM MgCl₂, cOmplete™ Mini EDTA-free protease inhibitor cocktail and PhosStop phosphatase inhibitors and incubated at 37°C for 30 min with 0.5 U/μl Benzonase™ Nuclease (all from Sigma-Aldrich). Sodium Dodecyl Sulfate (SDS) was added at a final concentration of 2% and cells were homogenized again. Protein extracts were centrifuged at 13,000 rpm for 10 min. Protein concentration of supernatants was estimated by the bicinchoninic acid assay (Sigma-Aldrich). Proteins (15 μg) were separated on NuPAGE™ 4-12% Bis-Tris Gel (Life Technologies) and electrophoretically transferred to nitrocellulose membranes (PROTAN™, Whatman GmbH). Membranes were incubated 3 hours with primary antibodies in PBS, 5% milk, 0.1% Tween 20, followed by one hour of incubation with appropriate secondary antibodies. Signals were detected using ECL™ Prime Western Blotting Detection Reagent (GE Healthcare Sa). Signal intensity was analyzed with MultiGauge 3.0 software.

2.5. Immunoprecipitation.

The whole procedure was done at 4°C. Proteins were extracted from cell pellets with a RIPA buffer: Tris-HCl pH8 (50 mM), NaCl (150 mM), NP40 (1%), sodium deoxycholate (12 mM) and protease and phosphatase inhibitors (Sigma-Aldrich). Protein extracts were centrifuged at 13,000 rpm for 10 min, and protein concentration of supernatants was quantified by the bicinchoninic acid assay (Sigma-Aldrich).

The lysates (200 µg of proteins) were pre-cleared by 30 min incubation on a rotated wheel with hNuclei antibody (mouse IgG1), an isotype/species matched irrelevant antibody to the immunoprecipitation antibody and then 1h with proteinG agarose beads (Sigma-Aldrich). Beads were spun down 3 min at 13,000 rpm. Supernatants were incubated with ubiquilin-2 antibody (mouse IgG1) and proteinG agarose 1h under rotation. Pellets were recovered and washed 6 times with RIPA buffer. Immunoprecipitated proteins were boiled in SDS sample buffer and processed for western blot analysis.

2.6. Statistical tests.

Statistical analyses were performed using GraphPad Prism software (v.6). Kruskal-wallis analysis of variance was used to compare densitometry data of control, P494L, P497S and P506A groups. Then, if this analysis showed a statistical difference, the non parametric Mann Whitney t-test was used to compare groups 2 by 2.

3. Results

3.1. Genetic analysis of French patients with motor neuron diseases revealed four novel *UBQLN2* mutations.

UBQLN2 genetic analysis revealed 5 *UBQLN2* mutations. The already reported c.1489C>T, p.Pro497Ser, P497S (Deng et al., 2011) was found in a family presenting ALS/FTD. Three novel *UBQLN2* missense mutations were also identified in familial cases: the c.1481C>T, p.Pro494Leu, P494L in ALS/FTD family, the c.1498C>T, p.Pro500Ser, P500S in FALS and the c.1516C>G, p.Pro506Ala, P506A in patients from a family with ALS and SP (Fig. 1A) with no other causing mutation in ALS and SP genes (screened using Gene-Panel sequencing approaches). We also identified the novel c.1462G>A, p.Ala488Thr, A488T missense mutation in a sporadic ALS case. All these mutations were absent from the Exome variant server NHLBI GO *Exome* Sequencing Project (ESP), the ExAC (Exome Aggregation Consortium) and gnomAD (Genome Aggregation Database) browsers (Lek et al., 2016) as well as from our own datasets of 380 control samples (age-matched Caucasian individuals of French background) and 400 exomes of spinocerebellar degeneration cases. These mutations affected

residues that were conserved in mammals (Fig. 1B) and were predicted to be deleterious by SIFT *in silico* analysis. As most ALS causing mutations identified in ubiquilin-2, 4 of these alterations affected a proline residue of the PXX tandem repeat region and the last one is located immediately adjacent to this domain (Fig. 1C).

3.2. Clinical description of the patients with *UBQLN2* mutation showed either ALS (\pm FTD) or SP.

The woman with the P497S mutation had bulbar onset ALS at 48y of age. Limbs tetraparesis remained moderate throughout disease course. Fasciculations were observed in upper limbs and tongue. Pyramidal signs attested by bilateral Babinski and Hoffmann signs appeared after 5 years of disease course. She died at 53y following 63 months of disease duration (one year after gastrostomy tube placement and a few months after FTD diagnosis). Her mother died before the age of 40y from a bulbar onset ALS disease with concomitant FTD. Her aunt developed bulbar onset ALS with age of death at around 30y. Her uncle also died of FTD-ALS.

The patient harboring the P494L mutation was a woman who first experienced at 55y a distal muscle weakness in the right hand, extending 6 months later to homolateral foot. Upper motor neuron signs (brisk reflex in four limbs and right Hoffman sign) were present. At 57y, her weakness progressed to contralateral distal lower limb muscles with moderate bulbar dysfunction but no respiratory muscle involvement. Lower motor neuron signs were observed in her four limbs with clear muscular atrophy and neurogenic pattern attested by electromyography (EMG). Bilateral Hoffmann and Babinski signs were present. Now aged 59y, she has no cognitive or behavioral dysfunction but is using nocturnal non invasive ventilation. The patient's eldest sister, an obligate carrier for the mutant X, is free of symptoms at 60y. A diagnosis of FTD was made for their father at the age of 69y, and was rapidly followed by a classical ALS clinical pattern associated with axial extrapyramidal signs. He died at 72y of head injury. Their paternal grand-mother, an obligate carrier, died at 80y without sign of motor neuron disease (Fig. 2A).

For the woman with the P500S mutation, weakness onset appeared in the right arm at 62y. She was first diagnosed with cervico-brachial neuralgia that was not relieved by a surgery for C5-C6 disc herniation. She was referred to an ALS disease center 9 months after the first symptoms. EMG showed signs of upper and lower motor neuron involvement that were detected for the 4 limbs and bulbar muscles. Bulbar function (phonation) rapidly worsened and she died from respiratory failure after 16 months of disease duration with no cognitive defect. Her mother developed a bulbar onset ALS at 75y (dysarthria and phonation) up to death after a rapid disease duration of 10 months (Fig. 2B). Index case's brother is healthy at 65y. Her grandfather died at 80y and her grandmother died at 28y from leukemia. Her uncles died at 78 and 81y of cancer and cardiac failure, respectively.

The index case with the P506A mutation was from a family including four male members over three generations who were affected by a motor neuron disease (Fig. 2C). Ten years after the onset of lower limb upper motor neuron signs (that occurred at 35y and led to the SP diagnosis), this patient developed an aggressive ALS disease with rapid lower motor neuron involvement and diffusion of upper motor neuron signs to bulbar and cervical regions resulting in tetraplegia within 12 months, associated to dysarthria and dysphagia, as well as diaphragmatic paralysis due to the degeneration of motor neurons in the spinal cord, the brainstem and the cortex. His brother developed a spastic gait at the age of 27y. Four years later he was wheelchair ridden due to SP, with a mild neurogenic bladder. Since then, symptoms have remained stable during 20 years with isolated upper motor neuron involvement restricted to lower limbs. Now aged 47y, he is still able to make some steps using the parallel bars but developed recent upper motor neuron signs in both arms. Their mother is a healthy obligate carrier aged 69y. Their grandfather developed a SP at 30y leading to paralysis of the legs and died at 76y from cardiac failure. Their granduncle died at 66y from an ALS disease (severe paralysis and amyotrophy of lower and upper limbs with anarthria).

The man with the A488T mutation presented with progressive proximal weakness of both lower limbs at 47y. Lower motor neuron signs were in foreground, with proximal muscle wasting, fasciculations in both

lower limbs, and tendon reflexes diminished or abolished in lower limbs. Plantar response was indifferent. He died at 51y after disease duration of 51 months. No other ALS case was reported in his family.

3.3. Ubiquilin 2 did not accumulate in patient lymphoblasts with *UBQLN2* mutation.

To study the functional impact of the novel *UBQLN2* mutations we identified, lymphoblastoid cell lines were established from lymphocytes for the ALS patients carrying the P494L (female) and P506A (male) mutations and compared to lymphoblastoid cell lines carrying the known pathogenic P497S mutation (female). Western blot analysis showed that all these mutations did not impact the ubiquilin-2 protein expression level in *UBQLN2* lymphoblasts compared to controls (Fig. 3A-B).

3.4. Newly discovered *UBQLN2* mutations led to impaired autophagy.

Autophagy disturbance was recently suggested to be involved in accumulation of polyubiquitinated substrates observed after the simultaneous overexpression of four *UBQLN2* mutations (P497H+P506T+P509S+P525S) in mouse neuroblastoma cell line (Osaka et al., 2016). Here we aimed to determine whether autophagy process was modified in patient lymphoblasts and analyzed the different states of LC3 protein. LC3-II, a marker of autophagosome formation/accumulation, is formed by the conjugation of the cytosolic LC3-I with phosphatidylethanolamine and is associated to the autophagosome. However even if its molecular weight is higher than that of LC3-I, LC3-II migrates faster in SDS-PAGE due to its hydrophobicity (Mizushima and Yoshimori, 2007). Levels of LC3-II autophagic marker were increased in patients with *UBQLN2* mutation compared to healthy controls (Fig. 3A&C). To confirm that autophagy process was impaired in lymphoblasts carrying *UBQLN2* mutations, we also analyzed basal levels of the autophagic substrate p62 (SQSTM1/sequestosome 1). Levels of p62 were upregulated in mutant *UBQLN2* lymphoblasts (Fig. 3A&D). Increase of both p62 and LC3-II suggested that autophagosomes accumulated either through induction of autophagosome formation or inhibition of autophagic degradation (Mizushima and Yoshimori, 2007). To discriminate between both

possibilities, we analyzed p62 and LC3-II levels in the presence of ammonium chloride (NH₄Cl), a lysosomal inhibitor that prevents lysosome acidification required for autophagosome-lysosome fusion. In contrast to control lymphoblasts that exhibited the expected increase in p62 and LC3-II levels after lysosomal inhibitor treatment, lymphoblasts with *UBQLN2* mutation did not further accumulate p62 (Fig. 4A) or LC3-II (Fig. 4B) indicating that defect in lysosome degradation was responsible for LC3-II/p62 accumulation observed in these cells.

3.5. *UBQLN2* mutations did not affect heat-shock induced upregulation of HSP70 but disrupted HSP70 binding.

As ubiquilin-2 was recently shown to interact with HSP70 (Hjerpe et al., 2016), we aimed to analyze HSP70 mediated response in patient's lymphoblasts carrying the *UBQLN2* mutations we identified. We first submitted lymphoblasts to heat-shock to analyze the level of HSP70. HSP70 protein levels were similar and similarly increased after heat-shock in lymphoblasts carrying or not a *UBQLN2* mutation (Fig. 5A-B, Fig 6C). However co-immunoprecipitation experiments using anti-*UBQLN2* antibodies revealed a disruption in HSP70 binding for ubiquilin-2 mutants (Fig. 6A-B).

As the HSP70 binding disruption was similar for the male (with hemizygous P506A mutation) and the female (with heterozygous P494L or P497S mutation) patients (Fig. 6B), we decided to sequence cDNA prepared from RNA lymphoblasts to analyze whether the normal X could be skewed in the female patients. Sanger electrofluorograms revealed that both ubiquilin-2 forms (mutant and non mutant) were present in the female lymphoblasts carrying the P494L or P497S mutation (Fig. 7).

4. Discussion.

We identified three novel *UBQLN2* mutations (P494L, P500S and P506A) in families with motor neuron diseases involving one proline residue of the PXX repeat, a hot spot domain for ALS mutations (Deng et al., 2011).

The segregation of the P506A mutation with the disease could be analyzed: the ALS patient's brother who was affected by SP also carried it. Notably the 2 brothers, for whom we could analyze the DNA, developed motor neuron disease before 35 years of age. Remarkably motor neuron disease only affected males in this P506A large pedigree. All daughters (n=9) and the mother from the 2 affected male ancestors, who are obligate carriers for the mutant X, remained all still asymptomatic at 60-70y and 13 of their 17 sons were also free of symptoms at 40-50y. The disease penetrance can thus be estimated as 0% (0/10) for females between 60-70y in this pedigree. Incomplete disease penetrance for *UBQLN2* mutations was occasionally reported for some asymptomatic females aged 50-90y but was previously estimated as around 80% (Deng et al., 2011; Vengoechea et al., 2013), and to our knowledge, the low disease penetrance we observed in the P506A pedigree has never been reported. This observation has to be taken into account before delivering a genetic counseling to the concerned families.

Two other mutations have been reported at the P506 amino acid position affected by our novel P506A mutation. The first one (P506T) was identified in FALS cases with early disease onset ranging from 25 to 44 y (Deng et al., 2011). The second one (P506S) was identified in FALS cases who developed ALS before 30y (Gellera et al., 2013; Ozoguz et al., 2015) and interestingly, in a large family with different presentations of motor neuron disease leading to different neurological diagnoses: ALS with upper motor neuron onset, ALS/FTD, primary lateral sclerosis, bulbar palsy and conflicting diagnoses including multiple sclerosis (Vengoechea et al., 2013). Atypical neurodegenerative disease combining early onset (at 5 to 20 years of age) SP, dysarthria, dysphagia and behavioral dementia in the descendants of a 67 year-old woman with ALS was also described in a multigenerational family carrying the P497L mutation (Fahed et al., 2014). In the P506A family we report here, 3 out of 4 affected members first manifested spasticity leading a SP diagnosis. This clinical pattern worsened to an unequivocal ALS disease for one of them. These observations suggest a predominant/primarily upper motor neuron dysfunction for patients carrying this P506A mutation.

Our results confirmed the role of ubiquilin-2 PXX repeat in ALS pathogenesis and expand the spectrum of *UBQLN2* mutations to an atypical SP phenotype with X-linked inheritance.

Experiments we performed on patient lymphoblasts showed that mutant forms of ubiquilin-2 were not downregulated or accumulated. However accumulation of autophagosomes in mutant lymphoblasts were evidenced by the increased levels of LC3-II and p62 displayed in our western blot analyses. This accumulation could be due to either a disruption of proteasome function (which is known to result in a compensatory autophagy induction) or to disruption of lysosomal function, since both of these processes increase LC3-II and p62 levels (Ding et al., 2007; Mizushima and Yoshimori, 2007; Korolchuk et al., 2009; Matsumoto et al., 2011; Lim et al., 2015). Impairment of UPS process has been described in cells overexpressing *UBQLN2* ALS mutations which accumulated UPS reporter substrate (Deng et al., 2011; Gorrie et al., 2014; Chang and Monteiro, 2015). However in our study, as no further increase of LC3-II and p62 occurred after treatment by the lysosomal inhibitor NH₄Cl in mutant lymphoblasts, autophagosome accumulation is, at least in part, the consequence of impaired lysosome degradation. The lysosome proteolysis disturbance we observed in *UBQLN2* mutant lymphoblasts is in line with previous studies showing that the depletion of ubiquilin proteins inhibited the degradation of autophagosomes by lysosomes (N'Diaye et al., 2009) and that *UBQLN2* mutants were delocalized from the autophagosome compartment (Osaka et al., 2016).

Co-immunoprecipitation experiments we performed on patient lymphoblasts showed that novel *UBQLN2* mutations impaired HSP70 binding. This result was not due to a downregulation of HSP70 levels in lymphoblasts expressing mutant *UBQLN2*, which were fully able to activate expression of HSP70 after being exposed to heat-shock. Our data importantly, obtained in patient cells, confirms the role of *UBQLN2* as shuttle factor for HSP70-bound substrates previously shown in stably transfected HEK293T cells and in mouse embryonic fibroblasts derived from constitutive knock-in mouse model (Hjerpe et al., 2016). The minimal *UBQLN2* sequence for heat-shock protein binding consisted of residues 319-520

(Kaye et al., 2000) which is intriguingly similar to the hot spot domain for ALS/FTD mutations (Fig. 1C). However, as the deletion of the PXX domain did not influence HSP70 binding, it was further suggested that PXX mutation could rather alter the optimal ubiquilin-2 conformation for HSP70 mediated response, preventing client-bound HSP70 protein delivery to the proteasome and leading to accumulation of aggregated and/or misfolded proteins in ALS disease (Hjerpe et al., 2016).

UBQLN2 is an X-linked gene subjected to X-inactivation (Carrel and Willard, 2005). The similar level of ubiquilin-2 protein that was actually detected for the female (with P494L or P497S mutation) and the male lymphoblasts (P506A mutation), argued in favor of the silencing of one X in the female lymphoblasts, equalizing the ubiquilin-2 protein level compared with the male. Nevertheless due to this X-inactivation process, we expected to observe a stronger impairment of HSP70 binding in male (P506A) than in female (P494L or P497S) mutant *UBQLN2* lymphoblasts having mutant X or the other one active. However this was not observed. An appealing explanation would have been that our female lymphoblasts expressed only the P494L/P497S mutant forms of *UBQLN2* due to tissue specific X skewing or to lymphoblasts themselves which may sometimes become clonal in culture (Migeon et al., 1988). However our sequencing experiments performed on cDNA prepared from P494L and P497S lymphoblasts showed that both mutant and normal *UBQLN2* alleles were expressed in our cultures rather suggesting that X-inactivation process occurred randomly in these cells. The level of expression of mutant *versus* normal *UBQLN2* should be further investigated in female post-mortem central nervous system tissue carrying *UBQLN2* mutations to determine the impact of X skewing on ALS disease penetrance and severity.

Another possible explanation relies on the ubiquilin-2 capability to form homodimers through the central region of the protein, independently of its UBL and UBA domains (Ford and Monteiro, 2006). As this process may regulate the ability to bind to other partners by preventing other protein interaction (Ford and Monteiro, 2006), our observations in female lymphoblasts could result from a dominant negative

effect of the mutant form of ubiquilin-2 trapping the normal ubiquilin-2 in such dimers. Whether dimerization/oligomerization of ubiquilin-2 is involved in ALS pathogenesis should be further investigated.

Our results confirmed the role of PXX repeat in ALS pathogenesis, showed that *UBQLN2*-linked motor neuron disease can manifest like an atypical SP phenotype and underlined a very low disease penetrance of P506A *UBQLN2* mutations in females, important information for genetic counseling. Our results also showed that PXX *UBQLN2* mutations impaired HSP70 binding and impacted autophagy pathway in patient cells. Taken together, our results and those from previous studies suggest that several protein degradation pathways are improperly regulated in patient cells with *UBQLN2* mutations and underline the pivotal role of ubiquilin-2 in proteolysis regulation.

Acknowledgments.

We acknowledge the patients and their family. We thank the Généthon cell and DNA bank (Evry, France) and the ICM DNA and cell bank (Paris, France) for patient DNA and lymphoblasts and the ICM CELIS core facilities (Paris, France) for cell equipment access. This study was funded by the Association Française contre les Myopathies (AFM, France, contract R16061DD), the Association pour la Recherche sur la Sclérose latérale amyotrophique et autres maladies du motoneurone (ARSLa, France, contract R17050DD), the Aide à la Recherche des Maladies du Cerveau association (ARMC, France, contract R16009DD) and a collaborative research program established between ICM, CHU de Limoges and Université de Limoges (ICM.SCI.1800.CRCO) to SM and by the Agence Nationale de la Recherche (PATAX-QUEST) and the Verum Foundation to GS. ET is supported by a PhD Fellowship from AFM (#18145).

References

- Brooks, B.R., Miller, R.G., Swash, M., Munsat, T.L., 2000. El Escorial revisited: revised criteria for the diagnosis of amyotrophic lateral sclerosis. *Amyotroph Lateral Scler Other Motor Neuron Disord* 1, 293-299.
- Carrel, L., Willard, H.F., 2005. X-inactivation profile reveals extensive variability in X-linked gene expression in females. *Nature* 434, 400-404.
- Chang, L., Monteiro, M.J., 2015. Defective Proteasome Delivery of Polyubiquitinated Proteins by Ubiquilin-2 Proteins Containing ALS Mutations. *PLoS One* 10, e0130162.
- Deng, H.X., Chen, W., Hong, S.T., Boycott, K.M., Gorrie, G.H., Siddique, N., Yang, Y., Fecto, F., Shi, Y., Zhai, H., Jiang, H., Hirano, M., Rampersaud, E., Jansen, G.H., Donkervoort, S., Bigio, E.H., Brooks, B.R., Ajroud, K., Sufit, R.L., Haines, J.L., Mugnaini, E., Pericak-Vance, M.A., Siddique, T., 2011. Mutations in UBQLN2 cause dominant X-linked juvenile and adult-onset ALS and ALS/dementia. *Nature* 477, 211-215.
- Ding, W.X., Ni, H.M., Gao, W., Yoshimori, T., Stolz, D.B., Ron, D., Yin, X.M., 2007. Linking of autophagy to ubiquitin-proteasome system is important for the regulation of endoplasmic reticulum stress and cell viability. *Am J Pathol* 171, 513-524.
- Fahed, A.C., McDonough, B., Gouvion, C.M., Newell, K.L., Dure, L.S., Bebin, M., Bick, A.G., Seidman, J.G., Harter, D.H., Seidman, C.E., 2014. UBQLN2 mutation causing heterogeneous X-linked dominant neurodegeneration. *Ann Neurol* 75, 793-798.
- Ford, D.L., Monteiro, M.J., 2006. Dimerization of ubiquilin is dependent upon the central region of the protein: evidence that the monomer, but not the dimer, is involved in binding presenilins. *Biochem J* 399, 397-404.
- Gasser, T., Finsterer, J., Baets, J., Van Broeckhoven, C., Di Donato, S., Fontaine, B., De Jonghe, P., Lossos, A., Lynch, T., Mariotti, C., Schols, L., Spinazzola, A., Szolnoki, Z., Tabrizi, S.J., Tallaksen, C.M., Zeviani, M., Burgunder, J.M., Harbo, H.F., 2010. EFNS guidelines on the molecular diagnosis of ataxias and spastic paraplegias. *Eur J Neurol* 17, 179-188.
- Gellera, C., Tiloca, C., Del Bo, R., Corrado, L., Pensato, V., Agostini, J., Cereda, C., Ratti, A., Castellotti, B., Corti, S., Bagarotti, A., Cagnin, A., Milani, P., Gabelli, C., Riboldi, G., Mazzini, L., Soraru, G., D'Alfonso, S., Taroni, F., Comi, G.P., Ticozzi, N., Silani, V., 2013. Ubiquilin 2 mutations in Italian patients with amyotrophic lateral sclerosis and frontotemporal dementia. *J Neurol Neurosurg Psychiatry* 84, 183-187.
- Gorrie, G.H., Fecto, F., Radzicki, D., Weiss, C., Shi, Y., Dong, H., Zhai, H., Fu, R., Liu, E., Li, S., Arrat, H., Bigio, E.H., Disterhoft, J.F., Martina, M., Mugnaini, E., Siddique, T., Deng, H.X., 2014. Dendritic spinopathy in transgenic mice expressing ALS/dementia-linked mutant UBQLN2. *Proc Natl Acad Sci U S A* 111, 14524-14529.
- Hjerpe, R., Bett, J.S., Keuss, M.J., Solovyova, A., McWilliams, T.G., Johnson, C., Sahu, I., Varghese, J., Wood, N., Wightman, M., Osborne, G., Bates, G.P., Glickman, M.H., Trost, M., Knebel, A., Marchesi, F., Kurz, T., 2016. UBQLN2 Mediates Autophagy-Independent Protein Aggregate Clearance by the Proteasome. *Cell* 166, 935-949.
- Hofmann, K., Falquet, L., 2001. A ubiquitin-interacting motif conserved in components of the proteasomal and lysosomal protein degradation systems. *Trends Biochem Sci* 26, 347-350.
- Kaye, F.J., Modi, S., Ivanovska, I., Koonin, E.V., Thress, K., Kubo, A., Kornbluth, S., Rose, M.D., 2000. A family of ubiquitin-like proteins binds the ATPase domain of Hsp70-like Stch. *FEBS Lett* 467, 348-355.
- Kenna, K.P., van Doornaal, P.T., Dekker, A.M., Ticozzi, N., Kenna, B.J., Diekstra, F.P., van Rheenen, W., van Eijk, K.R., Jones, A.R., Keagle, P., Shatunov, A., Sproviero, W., Smith, B.N., van Es, M.A., Topp, S.D., Kenna, A., Miller, J.W., Fallini, C., Tiloca, C., McLaughlin, R.L., Vance, C., Troakes, C., Colombrita, C., Mora, G., Calvo, A., Verde, F., Al-Sarraj, S., King, A., Calini, D., de Bellerocche, J., Baas, F., van der Kooij, A.J., de Visser, M., Ten Asbroek, A.L., Sapp, P.C., McKenna-Yasek, D., Polak, M., Asress, S., Munoz-Blanco, J.L., Strom, T.M., Meitinger, T., Morrison, K.E., Lauria, G., Williams, K.L., Leigh, P.N., Nicholson, G.A., Blair, I.P., Leblond, C.S.,

- Dion, P.A., Rouleau, G.A., Pall, H., Shaw, P.J., Turner, M.R., Talbot, K., Taroni, F., Boylan, K.B., Van Blitterswijk, M., Rademakers, R., Esteban-Perez, J., Garcia-Redondo, A., Van Damme, P., Robberecht, W., Chio, A., Gellera, C., Drepper, C., Sendtner, M., Ratti, A., Glass, J.D., Mora, J.S., Basak, N.A., Hardiman, O., Ludolph, A.C., Andersen, P.M., Weishaupt, J.H., Brown, R.H., Jr., Al-Chalabi, A., Silani, V., Shaw, C.E., van den Berg, L.H., Veldink, J.H., Landers, J.E., 2016. NEK1 variants confer susceptibility to amyotrophic lateral sclerosis. *Nat Genet* 48, 1037-1042.
- Kim, T.Y., Kim, E., Yoon, S.K., Yoon, J.B., 2008. Herp enhances ER-associated protein degradation by recruiting ubiquilins. *Biochem Biophys Res Commun* 369, 741-746.
- Kleijnen, M.F., Alarcon, R.M., Howley, P.M., 2003. The ubiquitin-associated domain of hPLIC-2 interacts with the proteasome. *Mol Biol Cell* 14, 3868-3875.
- Ko, H.S., Uehara, T., Tsuruma, K., Nomura, Y., 2004. Ubiquilin interacts with ubiquitylated proteins and proteasome through its ubiquitin-associated and ubiquitin-like domains. *FEBS Lett* 566, 110-114.
- Korolchuk, V.I., Mansilla, A., Menzies, F.M., Rubinsztein, D.C., 2009. Autophagy inhibition compromises degradation of ubiquitin-proteasome pathway substrates. *Mol Cell* 33, 517-527.
- Lek, M., Karczewski, K.J., Minikel, E.V., Samocha, K.E., Banks, E., Fennell, T., O'Donnell-Luria, A.H., Ware, J.S., Hill, A.J., Cummings, B.B., Tukiainen, T., Birbaum, D.P., Kosmicki, J.A., Duncan, L.E., Estrada, K., Zhao, F., Zou, J., Pierce-Hoffman, E., Berghout, J., Cooper, D.N., Deflaux, N., DePristo, M., Do, R., Flannick, J., Fromer, M., Gauthier, L., Goldstein, J., Gupta, N., Howrigan, D., Kiezun, A., Kurki, M.I., Moonshine, A.L., Natarajan, P., Orozco, L., Peloso, G.M., Poplin, R., Rivas, M.A., Ruano-Rubio, V., Rose, S.A., Ruderfer, D.M., Shakir, K., Stenson, P.D., Stevens, C., Thomas, B.P., Tiao, G., Tusie-Luna, M.T., Weisburd, B., Won, H.H., Yu, D., Altshuler, D.M., Ardissino, D., Boehnke, M., Danesh, J., Donnelly, S., Elosua, R., Florez, J.C., Gabriel, S.B., Getz, G., Glatt, S.J., Hultman, C.M., Kathiresan, S., Laakso, M., McCarroll, S., McCarthy, M.I., McGovern, D., McPherson, R., Neale, B.M., Palotie, A., Purcell, S.M., Saleheen, D., Scharf, J.M., Sklar, P., Sullivan, P.F., Tuomilehto, J., Tsuang, M.T., Watkins, H.C., Wilson, J.G., Daly, M.J., MacArthur, D.G., 2016. Analysis of protein-coding genetic variation in 60,706 humans. *Nature* 536, 285-291.
- Lim, J., Lachenmayer, M.L., Wu, S., Liu, W., Kundu, M., Wang, R., Komatsu, M., Oh, Y.J., Zhao, Y., Yue, Z., 2015. Proteotoxic stress induces phosphorylation of p62/SQSTM1 by ULK1 to regulate selective autophagic clearance of protein aggregates. *PLoS Genet* 11, e1004987.
- Matsumoto, G., Wada, K., Okuno, M., Kurosawa, M., Nukina, N., 2011. Serine 403 phosphorylation of p62/SQSTM1 regulates selective autophagic clearance of ubiquitinated proteins. *Mol Cell* 44, 279-289.
- Migeon, B.R., Axelman, J., Stetten, G., 1988. Clonal evolution in human lymphoblast cultures. *Am J Hum Genet* 42, 742-747.
- Millecamps, S., Corcia, P., Cazeneuve, C., Boillee, S., Seilhean, D., Danel-Brunaud, V., Vandenberghe, N., Pradat, P.F., Le Forestier, N., Lacomblez, L., Bruneteau, G., Camu, W., Brice, A., Meininger, V., LeGuern, E., Salachas, F., 2012a. Mutations in UBQLN2 are rare in French amyotrophic lateral sclerosis. *Neurobiol Aging* 33, 839.e831-833.
- Millecamps, S., Boillee, S., Le Ber, I., Seilhean, D., Teyssou, E., Giraudeau, M., Moigneu, C., Vandenberghe, N., Danel-Brunaud, V., Corcia, P., Pradat, P.F., Le Forestier, N., Lacomblez, L., Bruneteau, G., Camu, W., Brice, A., Cazeneuve, C., Leguern, E., Meininger, V., Salachas, F., 2012b. Phenotype difference between ALS patients with expanded repeats in C9ORF72 and patients with mutations in other ALS-related genes. *J Med Genet* 49, 258-263.
- Mizushima, N., Yoshimori, T., 2007. How to interpret LC3 immunoblotting. *Autophagy* 3, 542-545.
- N'Diaye, E.N., Kajihara, K.K., Hsieh, I., Morisaki, H., Debnath, J., Brown, E.J., 2009. PLIC proteins or ubiquilins regulate autophagy-dependent cell survival during nutrient starvation. *EMBO Rep* 10, 173-179.

- Osaka, M., Ito, D., Suzuki, N., 2016. Disturbance of proteasomal and autophagic protein degradation pathways by amyotrophic lateral sclerosis-linked mutations in ubiquilin 2. *Biochem Biophys Res Commun* 472, 324-331.
- Ozoguz, A., Uyan, O., Birdal, G., Iskender, C., Kartal, E., Lahut, S., Omur, O., Agim, Z.S., Eken, A.G., Sen, N.E., Kavak, P., Saygi, C., Sapp, P.C., Keagle, P., Parman, Y., Tan, E., Koc, F., Deymeer, F., Oflazer, P., Hanagasi, H., Gurvit, H., Bilgic, B., Durmus, H., Ertas, M., Kotan, D., Akalin, M.A., Gulluoglu, H., Zarifoglu, M., Aysal, F., Dosoglu, N., Bilguvar, K., Gunel, M., Keskin, O., Akgun, T., Ozcelik, H., Landers, J.E., Brown, R.H., Basak, A.N., 2015. The distinct genetic pattern of ALS in Turkey and novel mutations. *Neurobiol Aging* 36, 1764 e1769-1718.
- Rascovsky, K., Hodges, J.R., Knopman, D., Mendez, M.F., Kramer, J.H., Neuhaus, J., van Swieten, J.C., Seelaar, H., Dopper, E.G., Onyike, C.U., Hillis, A.E., Josephs, K.A., Boeve, B.F., Kertesz, A., Seeley, W.W., Rankin, K.P., Johnson, J.K., Gorno-Tempini, M.L., Rosen, H., Prileau-Latham, C.E., Lee, A., Kipps, C.M., Lillo, P., Piguet, O., Rohrer, J.D., Rossor, M.N., Warren, J.D., Fox, N.C., Galasko, D., Salmon, D.P., Black, S.E., Mesulam, M., Weintraub, S., Dickerson, B.C., Diehl-Schmid, J., Pasquier, F., Deramecourt, V., Lebert, F., Pijnenburg, Y., Chow, T.W., Manes, F., Grafman, J., Cappa, S.F., Freedman, M., Grossman, M., Miller, B.L., 2011. Sensitivity of revised diagnostic criteria for the behavioural variant of frontotemporal dementia. *Brain* 134, 2456-2477.
- Rothenberg, C., Srinivasan, D., Mah, L., Kaushik, S., Peterhoff, C.M., Ugolino, J., Fang, S., Cuervo, A.M., Nixon, R.A., Monteiro, M.J., 2010. Ubiquilin functions in autophagy and is degraded by chaperone-mediated autophagy. *Hum Mol Genet* 19, 3219-3232.
- Tesson, C., Koht, J., Stevanin, G., 2015. Delving into the complexity of hereditary spastic paraplegias: how unexpected phenotypes and inheritance modes are revolutionizing their nosology. *Hum Genet* 134, 511-538.
- Vengoechea, J., David, M.P., Yaghi, S.R., Carpenter, L., Rudnicki, S.A., 2013. Clinical variability and female penetrance in X-linked familial FTD/ALS caused by a P506S mutation in UBQLN2. *Amyotroph Lateral Scler Frontotemporal Degener* 14, 615-619.
- Walters, K.J., Kleijnen, M.F., Goh, A.M., Wagner, G., Howley, P.M., 2002. Structural studies of the interaction between ubiquitin family proteins and proteasome subunit S5a. *Biochemistry* 41, 1767-1777.
- Williams, K.L., Warraich, S.T., Yang, S., Solski, J.A., Fernando, R., Rouleau, G.A., Nicholson, G.A., Blair, I.P., 2012. UBQLN2/ubiquilin 2 mutation and pathology in familial amyotrophic lateral sclerosis. *Neurobiol Aging* 33, 2527 e2523-2510.
- Xia, Y., Yan, L.H., Huang, B., Liu, M., Liu, X., Huang, C., 2014. Pathogenic mutation of UBQLN2 impairs its interaction with UBXD8 and disrupts endoplasmic reticulum-associated protein degradation. *J Neurochem* 129, 99-106.

Figure legends

Fig. 1. Genetic analysis of French patients with motor neuron disease revealed four novel *UBQLN2* missense mutations.

(A) Part of electrofluorograms of *UBQLN2* showing the heterozygous c.1481C>T, p.Pro494Leu (P494L) and c.1498C>T, p.Pro500Ser (P500S) mutations and the hemizygous c.1462G>A, p.Ala488Thr (A488T) and c.1516C>G, p.Pro506Ala (P506A) mutations. (B) Sequence alignments of part of the *UBQLN2* amino acids between diverse species showing the evolutionary conservation of the Ala488, Pro494, Pro500 and Pro506 amino acids (boxed) among mammals. Sequences used include *Homo sapiens* ([NP_038472.2](#)), *Pan troglodytes* ([XP_003317539.1](#)), *Bos taurus* ([NP_001192611.1](#)), *Rattus norvegicus* ([NP_061268.2](#)), *Mus musculus* ([NP_001101721.1](#)). (C) The P494L, P500S and P506A mutations (red arrows) were localized in the PXX tandem repeat domain (in purple) where other ALS mutations have already been reported (black arrows). The A488T mutation (green arrow) is adjacent to this hot spot domain. Data are compiled from Deng et al. 2011, Williams et al. 2012, Gellera et al. 2013, Vengoechea et al. 2013, Fahed et al. 2014. The minimal sequence for heat-shock response was from Kaye et al. 2000. UBL: ubiquitin-like domain, ST11: heat-shock chaperonin-binding motif, UBA: ubiquitin-associated domain.

Fig. 2. Family disease history of the patients carrying the novel *UBQLN2* mutations.

Pedigrees of the patients carrying the c.1481C>T, p.Pro494Leu, P494L (**A**); c.1498C>T, p.Pro500Ser, P500S (**B**) and c.1516C>G, p.Pro506Ala, P506A (**C**) mutations. Index cases are pointed by an arrow. When available, the age of onset, site of onset, disease duration and age of death (brackets) are indicated above the symbol representing the patients. The genotypes are indicated for the cases with available DNA. Black fill: Amyotrophic Lateral Sclerosis (ALS) case, black half fill: Spastic Paraplegia (SP) case. Points: asymptomatic mutant X carriers (all daughters and mothers of male carriers). FTD: Frontotemporal Dementia.

Fig. 3. *UBQLN2* mutations lead to accumulation of autophagic markers.

Immunoblot analysis of protein extracts from lymphoblasts of 2 healthy controls (lanes 2 and 3) and ALS patients carrying the P497S (lane 1), P494L (lane 4) or P506A (lane 5) *UBQLN2* mutation using anti-ubiquilin-2, p62, LC3 and GAPDH antibodies (A). Densitometry analyses of ubiquilin-2 (B), LC3 (C) and p62 (D) protein levels for controls (white) and patients with P497S (black), P494L (dark grey) or P506A (light grey) mutation. Data are means +/- standard errors of the mean (sem) of 5 to 12 values from 3 to 5 independent experiments. *UBQLN2* (B) and p62 (D) levels were standardized to GAPDH levels and represented as percentage of the controls. Proportion of LC3-II (involved in autophagosome formation) is represented to that of total LC3 (C). * $p < 0.05$, ** $p < 0.01$, *** $p < 0.001$.

Fig. 4. *UBQLN2* mutations impair lysosomal functions.

Densitometric analysis of p62 (A) and LC3-II (B) induction performed on immunoblots from lymphoblasts of controls (white) and ALS patients (black) carrying the *UBQLN2* mutations (P494L, P497S or P506A mutations) after treatment with the NH_4Cl lysosomal inhibitor. Data are means +/- sem of 9 values from 3 independent experiments. * $p < 0.05$, *** $p < 0.001$.

Fig. 5. *UBQLN2* mutations do not impact HSP70 levels or fold induction after heat shock.

Immunoblot analysis of lymphoblast protein extracts from controls and ALS patients carrying the known P497S and the novel P494L or P506A *UBQLN2* mutations using anti-HSP70 and anti-GAPDH antibodies (A). Densitometry analyses of HSP70 fold induction after heat shock for controls (white) and ALS patients carrying the P497S (black), P494L (dark grey) or P506A (light grey) *UBQLN2* mutations (B). Data are means +/- sem of 3 to 9 values from 3 independent experiments. HSP70 levels were standardized to GAPDH levels.

Fig. 6. *UBQLN2* mutations impair ubiquilin-2 binding to HSP70.

Lymphoblast extracts from controls and ALS patients carrying the P497L, P494L or P506A *UBQLN2* mutation were immunoprecipitated (IP) or not (input) using an anti-*UBQLN2* antibody after being exposed to heat shock (A). Densitometry analyses of *UBQLN2*-immunoprecipitated HSP70 (B) or HSP70 levels before immunoprecipitation (C) for controls (white) and patients with P497S (black), P494L (dark grey) or P506A (light grey) mutations. Data (represented as percentage of the controls) are means \pm sem of 3 (for patients) or 8 (for controls) values from 3 to 4 independent experiments. * $p < 0.05$, ** $p < 0.01$.

Fig. 7. P494L and P497S female lymphoblasts express mutant and normal *UBQLN2* alleles.

Sequencing of the cDNA prepared from the female lymphoblasts carrying the c.1481C>T, p.Pro494Leu (P494L) or the c.1489C>T, p.Pro497Ser (P497S) mutations.

The mutations were detected at the heterozygous state showing that both *UBQLN2* alleles were expressed in these lymphoblasts.

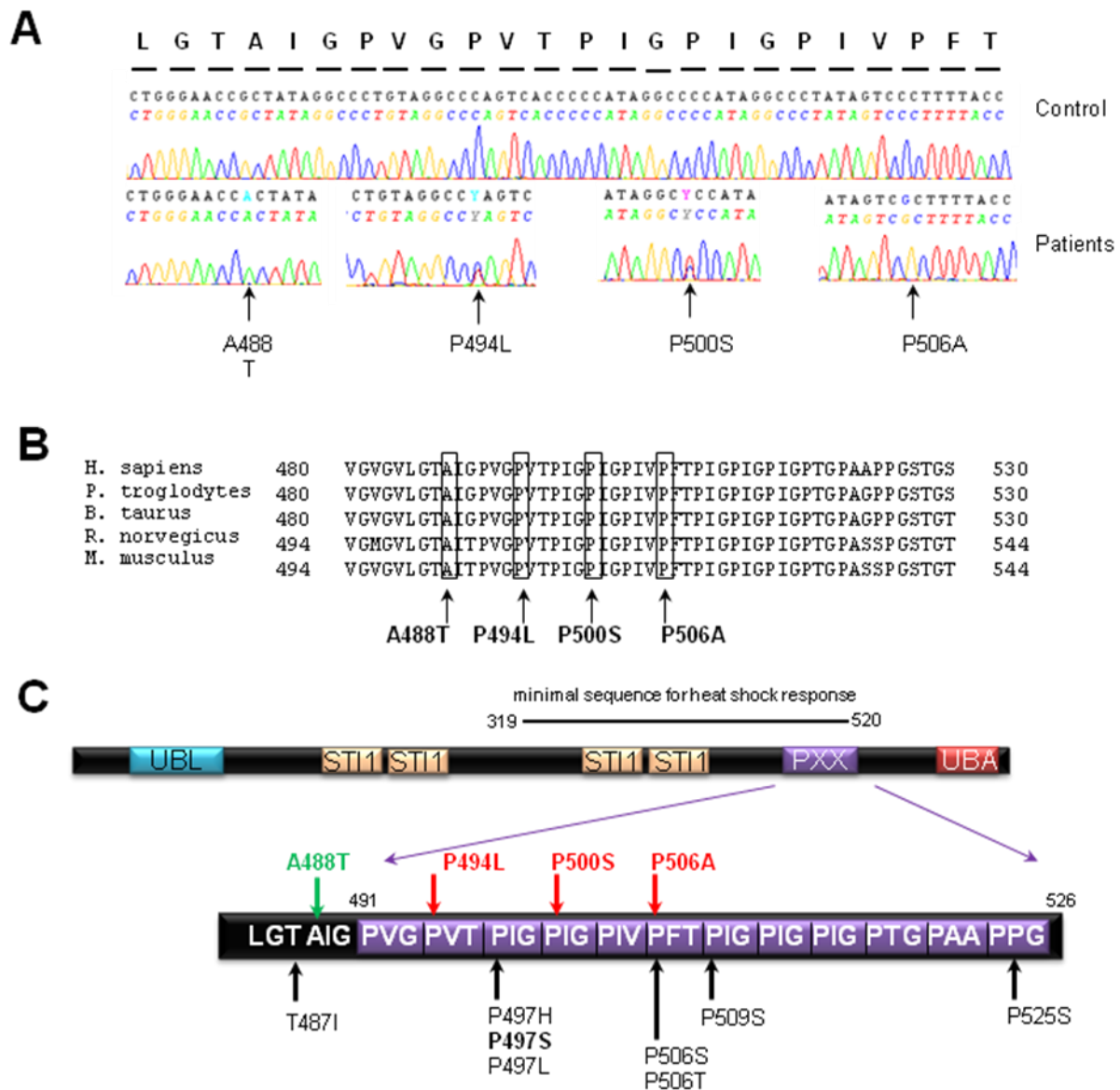


Fig. 1. Genetic analysis of French patients with motor neuron disease revealed four novel UBQLN2 missense mutations.

(A) Part of electrofluorograms of *UBQLN2* showing the heterozygous c.1481C>T, p.Pro494Leu (P494L) and c.1498C>T, p.Pro500Ser (P500S) mutations and the hemizygous c.1462G>A, p.Ala488Thr (A488T) and c.1516C>G, p.Pro506Ala (P506A) mutations. (B) Sequence alignments of part of the *UBQLN2* amino acids between diverse species showing the evolutionary conservation of the Ala488, Pro494, Pro500 and Pro506 amino acids (boxed) among mammals. Sequences used include *Homo sapiens* (NP_038472.2), *Pan troglodytes* (XP_003317539.1), *Bos taurus* (NP_001192611.1), *Rattus norvegicus* (NP_061268.2), *Mus musculus* (NP_001101721.1). (C) The P494L, P500S and P506A mutations (red arrows) were localized in the PXX tandem repeat domain (in purple) where other ALS mutations have already been reported (black arrows). The A488T mutation (green arrow) is adjacent to this hot spot domain. Data are compiled from Deng et al. 2011, Williams et al. 2012, Gellera et al. 2013, Vengoechea et al. 2013, Fahed et al. 2014. The minimal sequence for heat-shock response was from Kaye et al. 2000. UBL: ubiquitin-like domain, ST11: heat-shock chaperonin-binding motif, UBA: ubiquitin-associated domain.

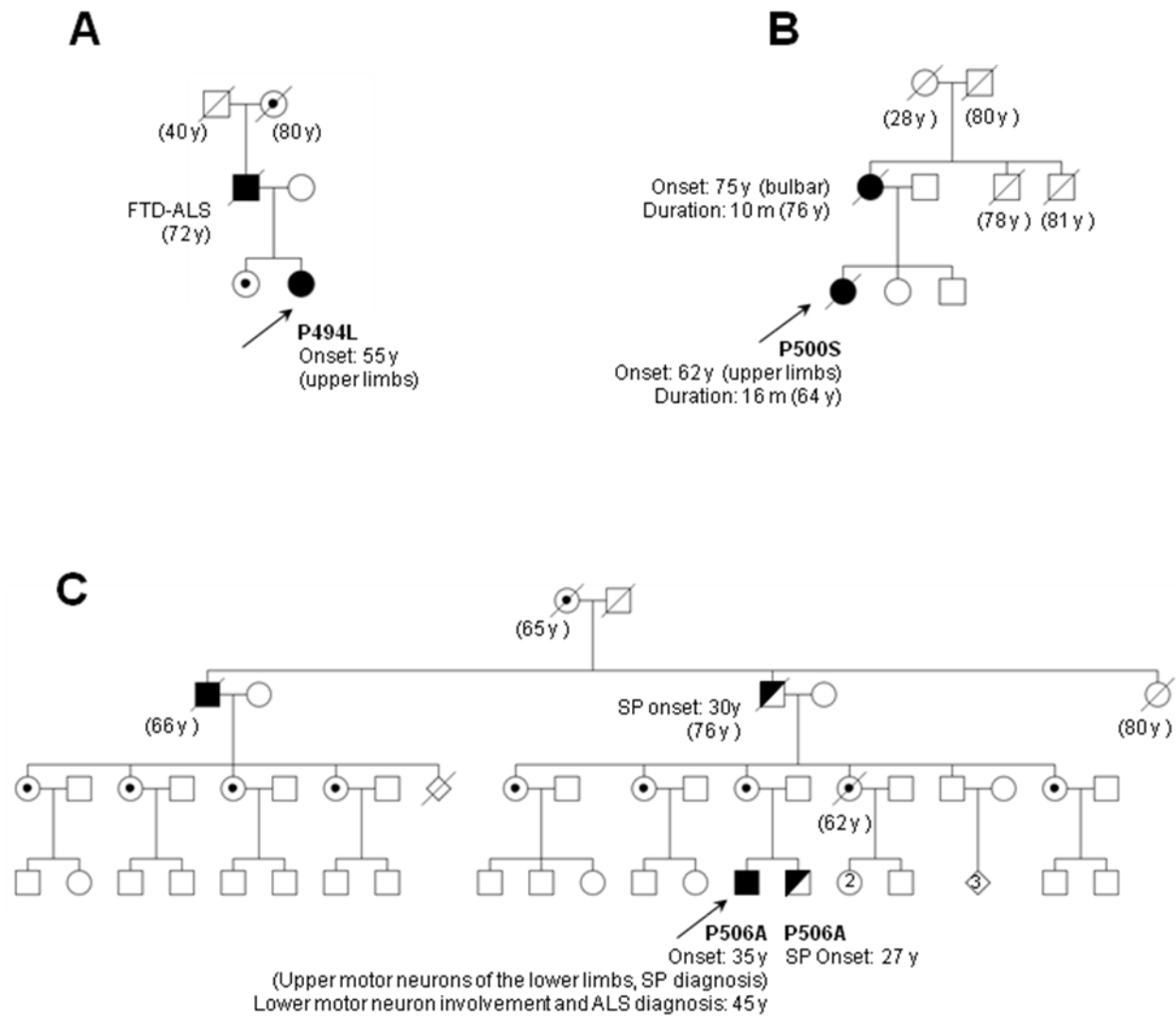


Fig. 2. Family disease history of the patients carrying the novel *UBQLN2* mutations. Pedigrees of the patients carrying the c.1481C>T, p.Pro494Leu, P494L (**A**); c.1498C>T, p.Pro500Ser, P500S (**B**) and c.1516C>G, p.Pro506Ala, P506A (**C**) mutations. Index cases are pointed by an arrow. When available, the age of onset, site of onset, disease duration and age of death (brackets) are indicated above the symbol representing the patients. The genotypes are indicated for the cases with available DNA. Black fill: Amyotrophic Lateral Sclerosis (ALS) case, black half fill: Spastic Paraplegia (SP) case. Points: asymptomatic mutant X carriers (all daughters and mothers of male carriers). FTD: Frontotemporal Dementia.

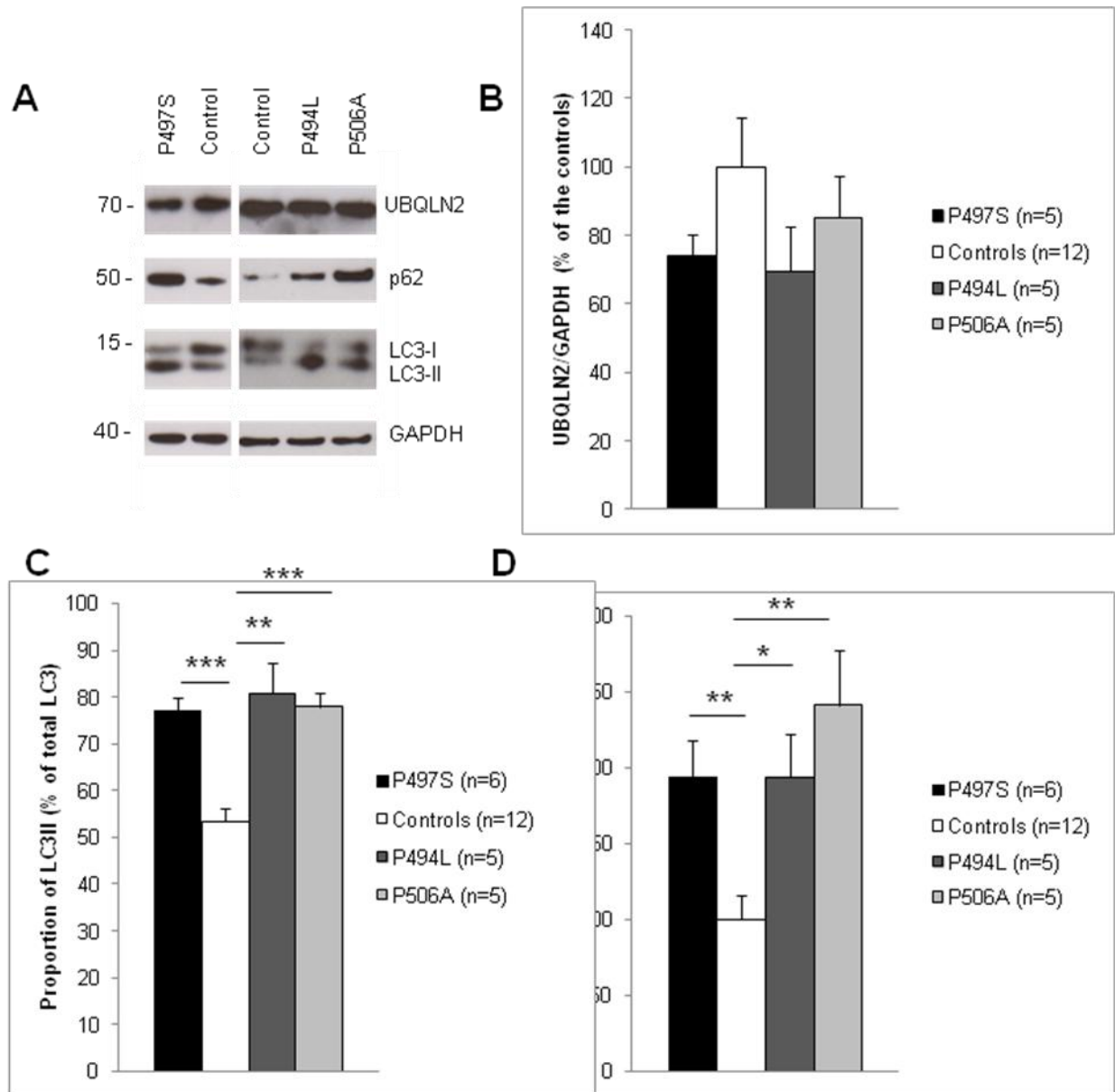


Fig. 3. UBQLN2 mutations lead to accumulation of autophagic markers.

Immunoblot analysis of protein extracts from lymphoblasts of 2 healthy controls (lanes 2 and 3) and ALS patients carrying the P497S (lane 1), P494L (lane 4) or P506A (lane 5) UBQLN2 mutation using anti-ubiquilin-2, p62, LC3 and GAPDH antibodies (A). Densitometry analyses of ubiquilin-2 (B), LC3 (C) and p62 (D) protein levels for controls (white) and patients with P497S (black), P494L (dark grey) or P506A (light grey) mutation. Data are means \pm standard errors of the mean (sem) of 5 to 12 values from 3 to 5 independent experiments. UBQLN2 (B) and p62 (D) levels were standardized to GAPDH levels and represented as percentage of the controls. Proportion of LC3-II (involved in autophagosome formation) is represented to that of total LC3 (C). * $p < 0.05$, ** $p < 0.01$, *** $p < 0.001$.

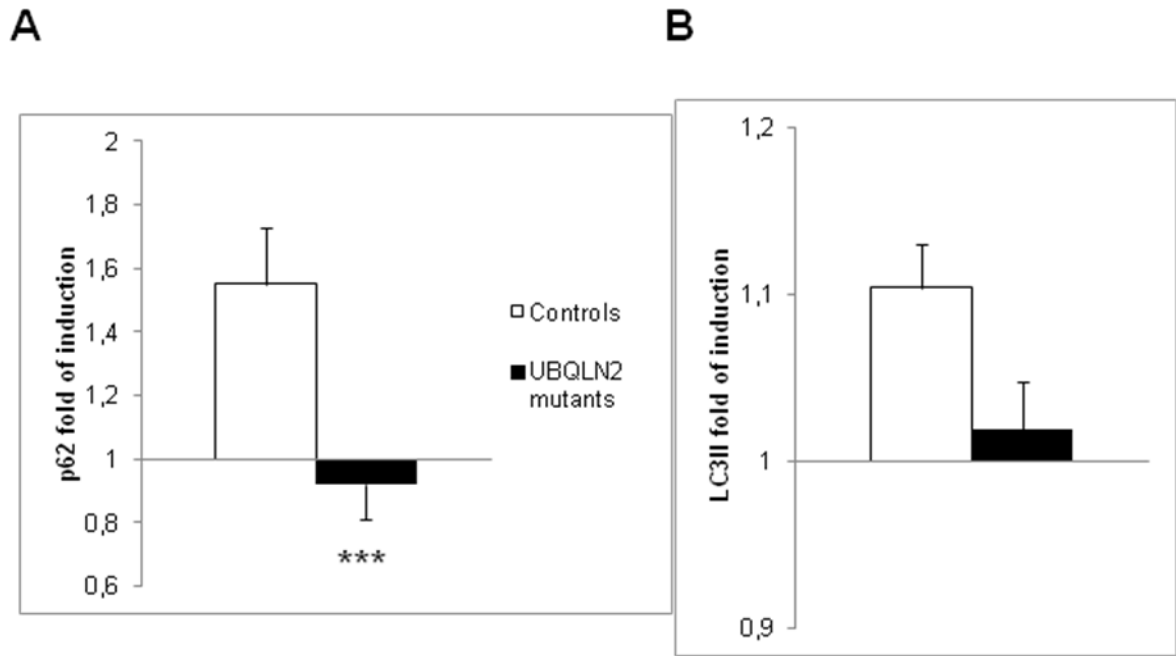


Fig. 4. UBQLN2 mutations impair lysosomal functions.

Densitometric analysis of p62 (A) and LC3-II (B) induction performed on immunoblots from lymphoblasts of controls (white) and ALS patients (black) carrying the *UBQLN2* mutations (P494L, P497S or P506A mutations) after treatment with the NH_4Cl lysosomal inhibitor. Data are means \pm sem of 9 values from 3 independent experiments. * $p < 0.05$, *** $p < 0.001$.

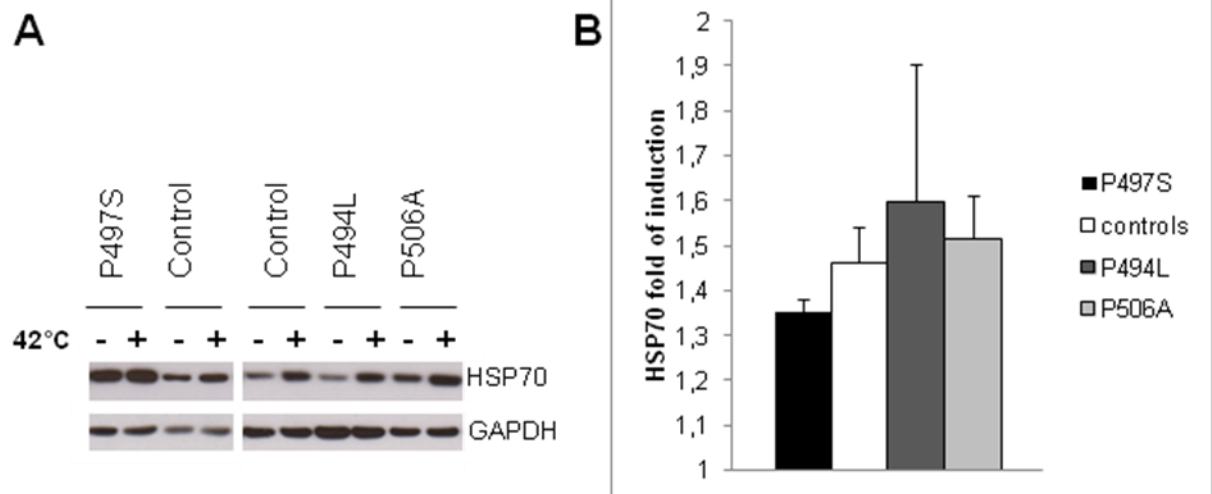


Fig. 5. *UBQLN2* mutations do not impact HSP70 levels or fold induction after heat shock.

Immunoblot analysis of lymphoblast protein extracts from controls and ALS patients carrying the known P497S and the novel P494L or P506A *UBQLN2* mutations using anti-HSP70 and anti-GAPDH antibodies (**A**). Densitometry analyses of HSP70 fold induction after heat shock for controls (white) and ALS patients carrying the P497S (black), P494L (dark grey) or P506A (light grey) *UBQLN2* mutations (**B**). Data are means \pm sem of 3 to 9 values from 3 independent experiments. HSP70 levels were standardized to GAPDH levels.

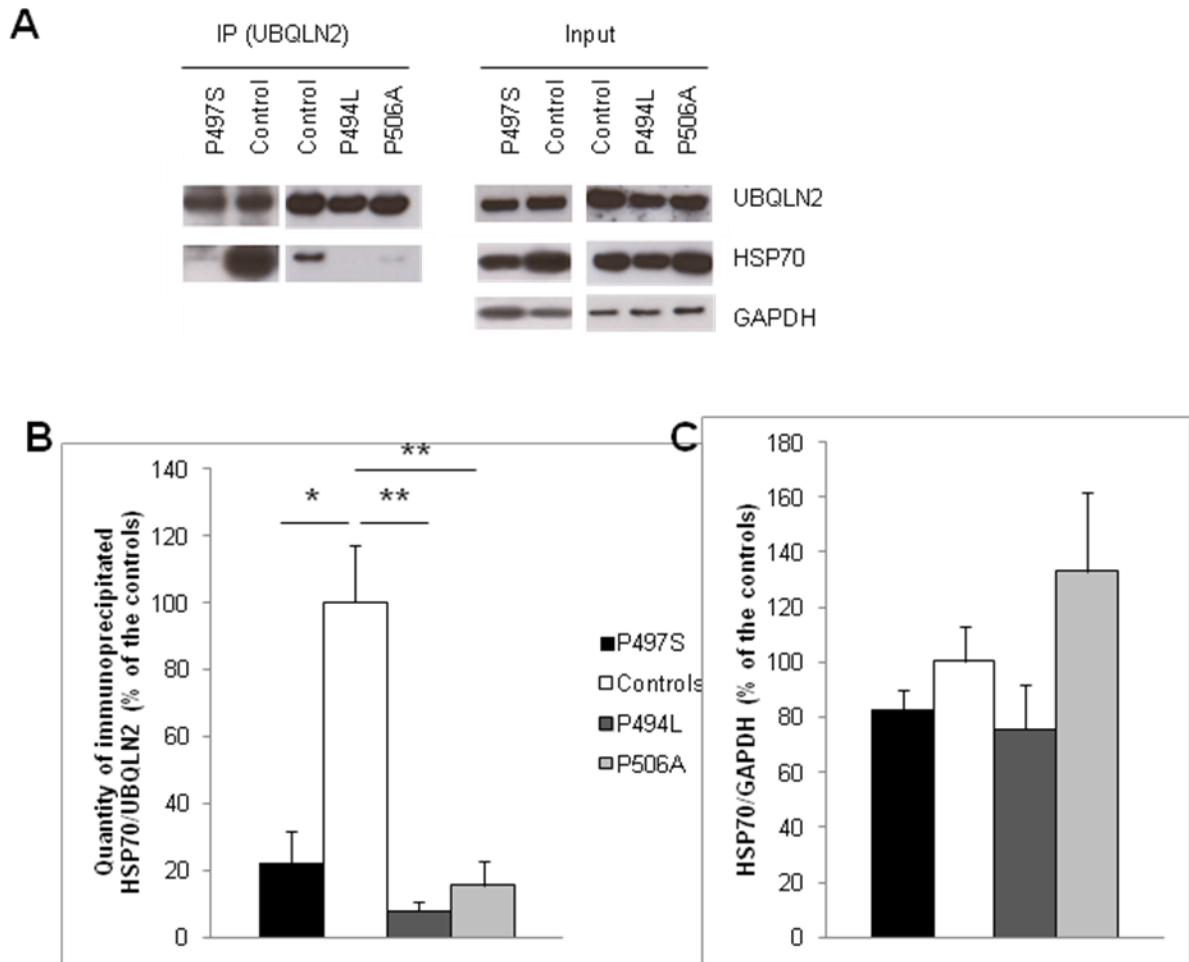


Fig. 6. UBQLN2 mutations impair ubiquitin-2 binding to HSP70.

Lymphoblast extracts from controls and ALS patients carrying the P497L, P494L or P506A UBQLN2 mutation were immunoprecipitated (IP) or not (input) using an anti-UBQLN2 antibody after being exposed to heat shock (A). Densitometry analyses of UBQLN2-immunoprecipitated HSP70 (B) or HSP70 levels before immunoprecipitation (C) for controls (white) and patients with P497S (black), P494L (dark grey) or P506A (light grey) mutations. Data (represented as percentage of the controls) are means +/- sem of 3 (for patients) or 8 (for controls) values from 3 to 4 in dependent experiments. * $p < 0.05$, ** $p < 0.01$.

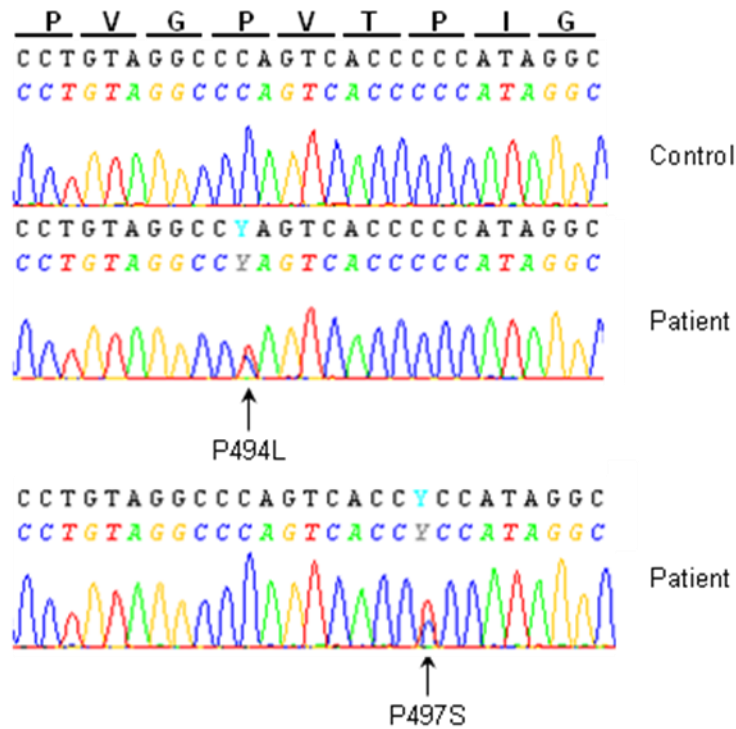


Fig. 7. P494L and P497S female lymphoblasts express mutant and normal *UBQLN2* alleles.

Sequencing of the cDNA prepared from the female lymphoblasts carrying the c.1481C>T, p.Pro494Leu (P494L) or the c.1489C>T, p.Pro497Ser (P497S) mutations.

The mutations were detected at the heterozygous state showing that both *UBQLN2* alleles were expressed in these lymphoblasts.